G protein-coupled oestrogen receptor activation by Bisphenol-A disrupts protection from apoptosis conferred by oestrogen receptors ERα and ERβ in pancreatic beta cells

Ignacio Babiloni-Chust[1,2,*], Reinaldo S. dos Santos[1,2,*], Regla M. Medina-Gali[1,2], Atenea A. Perez-Serna[1,2], José-Antonio Encinar[1], Juan Martinez-Pinna[3,1], Jan-Ake Gustafsson[4,5], Laura Marroqui[1,2] and Angel Nadal[1,2]

1. Instituto de Investigación, Desarrollo e Innovación en Biotecnología Sanitaria de Elche (IDiBE), Universidad Miguel Hernández de Elche, Elche, Spain.
2. Centro de Investigación Biomédica en Red de Diabetes y Enfermedades Metabólicas Asociadas (CIBERDEM), Spain. www.ciberdem.org
3. Departamento de Fisiología, Genética y Microbiología, Universidad de Alicante, Alicante, Spain.
4. Department of Cell Biology and Biochemistry, Center for Nuclear Receptors and Cell Signaling, University of Houston, Houston, TX, USA.
5. Department of Biosciences and Nutrition, Karolinska Institutet, Huddinge, Sweden

* Ignacio Babiloni-Chust and Reinaldo S. dos Santos contributed equally to this work.

Corresponding author

Angel Nadal, Instituto de Investigación, Desarrollo e Innovación en Biotecnología Sanitaria de Elche (IDiBE), Universitas Miguel Hernández, 03202, Elche, Spain.
E-mail: nadal@umh.es

ORCID identifiers

Ignacio Babiloni-Chust:
Regla M. Medina-Gali: 0000-0001-9401-8292
Atenea A. Perez-Serna: 0000-0002-7594-6365
Reinaldo S. dos Santos: 0000-0002-3219-4730
José A. Encinar: 0000-0002-7219-3863
Juan Martinez-Pinna: 0000-0003-0777-2049
Jan-Ake Gustafsson:
Laura Marroqui: 0000-0003-2931-9317

Angel Nadal: 0000-0003-4178-2152

Abbreviations

BERKO: Oestrogen Receptor β knockout

BPA: Bisphenol-A

DCF: 2',7'-Dichlorofluorescein diacetate

E2: 17β-oestradiol

ER: Oestrogen receptor

ERα: Oestrogen receptor α

ERβ: Oestrogen receptor β

GPER: G protein-coupled oestrogen receptor

LBD: Ligand binding domain

MPP: Methylpiperidinopyrazole

PHTPP: 4-(2-phenyl-5,7-bis(trifluoromethyl)pyrazolo[1,5-a]pyrimidin-3-yl)phenol

PLA: Proximity ligand assay

ROS: Reactive oxygen species

siRNA: Small interfering RNA

Abstract

Aims/hypothesis: 17β-oestradiol protects pancreatic beta cells from apoptosis via the oestrogen receptor α (ERα) and β (ERβ), and the G protein-coupled oestrogen receptor (GPER/GPR30). Conversely, the endocrine disruptor Bisphenol-A (BPA), which exerts multiple effects in beta cells via the same oestrogen receptors, increased basal apoptosis. We investigated the molecular initiated events underlying these opposite actions.

Methods: Apoptosis was determined by nuclear dyes, flow cytometry and luminescence. Oestrogen receptors were inhibited by small interfering RNAs. ERα and ERβ heterodimers were studied by molecular dynamics simulations, proximity ligand assay and co-immunoprecipitation. All experiments were performed in rat INS-1E and human EndoC-βH1 cells and dispersed islet cells from wild-type and ERβ knockout mice.

Results: BPA exposure induced reactive oxygen species production and induced apoptosis. GPER agonist G1 also induced apoptosis, but to a less extent than BPA. Either gene downregulation or pharmacological inhibition of each receptor resulted in augmented beta cell apoptosis in the absence of external stimuli. BPA- and G1-induced apoptosis was abolished in ERα-, ERβ- and GPER-silenced cells as well as in dispersed islet cells from ERβ knockout mice. Moreover, pharmacological blockade of each receptor also abrogated BPA- and G1-induced apoptosis. ERα and ERβ pharmacological agonists had no effect on beta cell viability. BPA interaction with ERα and ERβ as well as GPER activation by G1 or BPA decreased ERαβ heterodimerization.

Conclusions/interpretation: Our data suggest that ERα, ERβ and GPER play a key role in beta cell survival, where BPA-induced changes in GPER activation as well as in ERαβ heterodimer formation may increase beta cell apoptosis.

Keywords

Apoptosis, Bisphenol-A, Endocrine disruptors, GPER/GPR30, Heterodimers, 17β-oestradiol, Oestrogen receptors.

Research in context

What is already known about this subject?

- 17β-oestradiol protects beta cells from apoptosis via oestrogen receptors ERα, ERβ and GPER/GPR30
- Low doses of the xenoestrogen Bisphenol-A increase beta cell apoptosis

What is the key question?

- What is the role of the three oestrogen receptors on BPA-induced beta cell apoptosis?

What are the new findings?

- Pharmacological blockade and gene silencing of each receptor indicate that they are antiapoptotic in basal conditions.
- GPER activation by G1 and BPA triggered apoptosis via a crosstalk with ERα and ERβ.
- BPA interaction with ERα and ERβ and GPER activation decreased ERαβ heterodimers, which was associated to an increase in apoptosis.

How might this impact on clinical practice in the foreseeable future?

- Unveiling how different ligands affect the crosstalk among oestrogen receptors should help to understand their roles on beta cell survival and to develop new therapies based on oestrogen receptor regulation.

Introduction

Loss of functional beta cell mass is a critical component contributing to the hyperglycaemia observed in individuals with type 1 or type 2 diabetes. The interaction between the individual genetic background and environmental factors determines the progression of beta cell dysfunction and death [1].

Sex differences exist in the prevalence of diabetes. Premenopausal women have a lower incidence of diabetes compared with men [2, 3]. After a meal, insulin secretion is higher in women than in men [4], while islets isolated from female human donors and female rats secrete more insulin in response to glucose than male islets [5, 6]. These sex differences can be partially attributed to the actions of 17β-oestradiol (E2) through three oestrogen receptors (ERs), namely oestrogen receptors α (ERα) and β (ERβ) [7] and the G protein-coupled oestrogen receptor (GPER/GPR30) [8, 9]. After ligand binding, ERα and ERβ can either form homo- and heterodimers and act as transcription factors or tether other DNA-bound transcription factors [7]. In addition to their nuclear-initiated actions, ERα and ERβ can trigger extranuclear-initiated effects after dimerization and activate a variety of signalling pathways [10].

All three ERs protect beta cells from different apoptotic insults [11–13], yet the role of E2 can be disrupted by environmental chemicals that compete for the same receptors and modify the physiological pathways activated by the natural hormone [14]. Bisphenol-A (BPA), which is used as a model of endocrine disrupting chemical that alters insulin secretion and insulin sensitivity in mice [15, 16], has been implicated in the aetiology of diabetes [19,20]. At concentrations similar to those found in human blood [19], BPA increases pancreatic insulin content via ERα [20] and regulates ion channel expression and function as well as augments insulin release in an ERβ-mediated manner [21–23]. In INS-1 cells and mouse dispersed islet cells, BPA induces mitochondrial dysfunction, ROS production and NF-κB activation, which culminates in beta cell apoptosis [24, 25].

As E2 and BPA have opposite effects on beta cell survival, we decided to investigate the molecular mechanisms underlying BPA pro-apoptotic effects that could help to explain the differences between BPA and E2. Here we show that ERα, ERβ and GPER mediate beta cell survival. Our findings suggest that ERαβ heterodimerization is key to this antiapoptotic role and that G1, a GPER agonist, and BPA induce apoptosis via a mechanism involving the reduction in ERαβ heterodimers downstream of GPER.

Methods

For detailed methods, please refer to the electronic supplementary material (ESM).

Chemical substances and animals

The chemical substances used herein are described in the ESM Methods.

Mice with knockout of the *Erβ* gene (also known as *Esr2*) (BERKO mice), supplied by Jan-Åke Gustafsson's laboratory, were generated as described [26]. Wild-type littermates and BERKO mice were obtained from the same supplier and colony and kept under standard housing conditions (12 h light/dark cycle, food *ad libitum*). Experimental procedures were performed according to the Spanish Royal Decree 1201/2005 and the European Community Council directive 2010/63/EU. The ethical committee of Miguel Hernandez University reviewed and approved the methods used herein (approvals ID: UMH-IB-AN-01–14 and UMH-IB-AN-02-14).

Culture of cell lines and dispersed islet cells

Rat insulin-producing INS-1E cells (RRID: CVCL_0351, kindly provided by Dr. C. Wollheim, Department of Cell Physiology and Metabolism, University of Geneva, Geneva, Switzerland) were cultured as previously described [27]. Human insulin-producing EndoC-βH1 cells (RRID: CVCL_L909, Univercell-Biosolutions, France) were cultured in Matrigel/fibronectin-coated plates as described before [28]. INS-1E and EndoC-βH1 cells have been shown to be free of mycoplasma infection. Pancreatic islets were isolated using collagenase (Sigma, St Louis, MO, USA) as described [20]. Islets were dispersed into single cells and cultured in polylysine-coated plates as described before [21]. Cell lines and dispersed cells were kept at 37°C in a humidified atmosphere of 95% O_2 and 5% CO_2. See ESM Methods.

RNA interference

Optimal siRNA concentration (30 nmol/l) and conditions for small interfering RNA (siRNA) transfection using Lipofectamine RNAiMAX lipid reagent (Invitrogen, Carlsbad, CA, USA) were previously established [27]. Allstars Negative Control siRNA (Qiagen, Venlo, the Netherlands) was used as a negative control (siCTRL). siRNA targeting *Erα* (also known as *Esr1*; si*ERα*), *Erβ* (si*ERβ*) or *Gper1* (si*GPER1*) (Qiagen, Venlo, the Netherlands) were used herein (ESM Table 2). See ESM Methods.

Cell viability assessment by DNA-binding dyes

Percentage of apoptosis was determined after staining with the DNA-binding dyes Hoechst 33342 and propidium iodide as described [27]. See ESM Methods.

Flow cytometric analysis

Apoptotic cells were analysed by flow cytometry using the FITC Annexin V Apoptosis Detection Kit with propidium iodide (BioLegend, San Diego, CA, USA) following the manufacturer's instructions. Samples were analysed using a FACSCanto II (BD Biosciences, Madrid, Spain) flow cytometer. See ESM Methods.

Caspase 3/7 activity

Caspase 3/7 activity was determined using the Caspase-Glo® 3/7 assay (Promega, Madison, WI, USA) following the manufacturer's instructions. Briefly, following treatment, cells were incubated with Caspase-Glo® 3/7 reagent at room temperature before recording luminescence with a POLASTAR plate reader (BMG Labtech, Germany).

DCF assay

Oxidative stress was measured using the fluorescent probe 2',7'-dichlorofluorescein diacetate (DCF; Sigma-Aldrich) as described [29]. Briefly, cells seeded in 96-well black plates were loaded with 10 μmol/l DCF for 30 min at 37°C and washed with PBS. DCF fluorescence was quantified in a POLASTAR plate reader (BMG Labtech, Germany). Data are expressed as DCF fluorescence corrected by total protein.

Western blot

Cells were washed with ice-cold PBS and then lysed in Laemmli buffer. Immunoblot analysis was performed with the antibodies against ERα, ERβ and GPER listed in ESM table 1. See ESM Methods.

In situ proximity ligation assay (PLA)

In situ PLA was performed using a Duolink® In Situ Red Starter Kit (Sigma-Aldrich) following the manufacturer's instructions with slight modifications [30]. ER dimers were observed using a Zeiss Confocal LSM900 microscope equipped with a camera (Zeiss-

Vision, Munich, Germany) and images were acquired at x63 magnification and analysed using ZEN software (version 3.2; Zeiss-Vision, Munich, Germany). See ESM Methods.

Co-immunoprecipitation assay

Cells were lysed and total protein was co-immunoprecipitated using antibodies against ERβ and IgG (as a negative control). See ESM Methods.

Molecular docking and dynamics simulations

More than 300 human ERα-ligand-binding domain (LBD) (UniProt code: P03372) and 32 human ERβ-LBD (UniProt code: Q92731) structures were resolved from cryptographic data. As these structures contained unresolved residues in mobile regions of the protein that diffracted poorly, the lost amino acids were reconstructed after generation of a homology model at the Swiss-Model server [22, 31]. After unresolved gaps elimination, models for the hERα-LBD monomer (Protein Data Bank entry 5DXE as template) and the hERβ-LBD monomer (Protein Data Bank entry 3OLS as template) were generated. From these monomeric structures homo- and heterodimers were reconstructed using GRAMM-X server [32]. E2 and BPA molecular docking simulations within the cavity of each LBD were performed using the YASARA structure software (version 20.12.24) [22]. Molecular dynamics simulations on the structures with the best docking calculations were performed with YASARA structure software (version 20.10.24) [22]. The intermolecular protein interaction energy for homo- and heterodimers subunits was calculated using the Folds 5.0 software [33].

Statistical analysis

Experimenters were not blind to group assignment and outcome assessment. GraphPad Prism 7.0 software (GraphPad Software, La Jolla, CA, USA; www.graphpad.com) was used for all statistical analyses. Data are expressed as the mean ± SEM. To assess differences between groups, we used two-tailed Student's *t* test or ANOVA when appropriate. For nonparametric data we used Mann–Whitney and Kruskal–Wallis ANOVA tests (followed by Dunn's test), depending on the experimental groups involved in the comparison. A p value ≤ 0.05 was considered statistically significant.

Results

In INS-1E (Fig. 1a) and EndoC-βH1 cells (Fig. 1b), E2 (10 pmol/l to 1 μmol/l) either had no effect or decreased apoptosis. Conversely, BPA increased apoptosis in both cell lines in a dose-dependent manner (Fig. 1c,d). Similar results were observed in dispersed islet cells from female mice (Fig. 1e). These results were confirmed by three other approaches, namely flow cytometry analysis (Fig. 1f), caspase 3/7 activity (Fig. 1g) and MTT assay (ESM Fig. 1). When E2 and BPA were added together, E2 1 nmol/l prevented BPA-induced apoptosis (Fig. 1h), suggesting that E2 and BPA initiate common pathways.

Previous work demonstrated that BPA induces oxidative stress in beta cells [24, 25]. Similarly, we observed that BPA upregulated genes encoding the antioxidant enzymes, superoxide dismutase (*Sod2*), glutathione peroxidase 4 (*Gpx4*) and catalase (*Cat*) (ESM Fig. 2a-c) and increased reactive oxygen species (ROS) generation (ESM Fig. 2d,e). The antioxidant N-acetylcysteine abolished BPA-induced ROS production in INS-1E (ESM Fig. 2d) and EndoC-βH1 cells (ESM Fig. 2e). Notably, N-acetylcysteine prevented BPA-induced apoptosis in both cell lines (ESM Fig. 2f,g), reinforcing that oxidative stress is involved in BPA-induced apoptosis. Of note, E2 did not change ROS levels (data not shown).

As previous results indicate that BPA acts via ERs in beta cells [20, 21, 23] we evaluated the expression of ERα, ERβ and GPER in INS-1E and EndoC-βH1 cells by quantitative RT-PCR and western blot. Considering ERα expression as 1, mRNA analyses showed that the ratio GPER:ERα:ERβ was 100:1:0.3 for INS-1E (ESM Fig. 3a) and 675:1:3.3 for EndoC-βH1 cells (ESM Fig. 3b). This expression pattern was confirmed at protein level, where GPER was the most expressed of the three receptors (ESM Fig. 3c).

GPER mediates BPA-induced apoptosis

We first assessed whether GPER participated in BPA-induced apoptosis. GPER antagonist G15 reduced BPA-triggered apoptosis in INS-1E and EndoC-βH1 cells (Fig. 2a,b). Doses as low as 100 pM of the GPER agonist G1 induced apoptosis in INS-1E cells (ESM Fig. 4a). In comparison with BPA 1 nmol/l, G1 100 nmol/l presented a significantly smaller effect on apoptosis in both cell lines (Fig. 2c,d). To further study the GPER role in beta cell survival, we used siRNAs to inhibit GPER expression in INS-1E and EndoC-βH1 cells (Fig. 2e-j, ESM Fig. 4b,c). GPER silencing promoted apoptosis in basal conditions in INS-1E but not in EndoC-βH1 cells (Fig. 2f,i). Moreover, GPER-inhibited cells were less susceptible to BPA-induced apoptosis than control cells (Fig. 2f,g,i,j).

Similar data were obtained with a second, independent siRNA (data not shown). These results indicate that GPER activation is part of the mechanism whereby BPA elicits apoptosis.

ERα and ERβ are involved in BPA-induced apoptosis

We then investigated whether ERα and ERβ were also implicated in BPA-induced apoptosis. In both cell lines, the pure antioestrogen ICI 182,780 abolished the BPA effect on apoptosis (Fig. 3a,b). Treatment with the ERα antagonist methylpiperidinopyrazole (MPP) induced apoptosis in basal conditions, while propylpyrazoletriol,(PPT) an ERα agonist, did not change viability (Fig. 3c, ESM Fig. 5a,b). In INS-1E cells, MPP abolished BPA-induced apoptosis (Fig. 3c). To further characterize ERα participation in cell survival and BPA-induced apoptosis, we silenced ERα expression in INS-1E and EndoC-βH1 cells using specific siRNAs (Fig. 3d,g, ESM Fig. 5c-e). ERα knockdown augmented apoptosis in basal conditions and prevented BPA-induced apoptosis in both cell lines (Fig. 3e,f,h,i). We confirmed these data with a second, independent siRNA (data not shown).

Regarding ERβ, while its antagonist 4-(2-phenyl-5,7-bis(trifluoromethyl)pyrazolo[1,5-a]pyrimidin-3-yl)phenol (PHTPP) also induced apoptosis in basal conditions, ERβ agonist diarylpropionitrile (DPN) had no effect on beta cell viability (Fig. 4a, ESM Fig. 6a,b). ERβ inhibition by siRNAs (Fig. 4c,f, ESM Fig. 6c-h) induced a substantial increase in apoptosis, mainly in INS-1E cells; importantly, BPA-elicited apoptosis was partially lost following ERβ silencing (Fig. 4d,e,g,h). Comparable results were observed with a second, independent siRNA (data not shown). Finally, BPA effects on viability were abrogated in dispersed islets cells from BERKO (Fig. 4b).

A crosstalk among ERα, ERβ and GPER mediates beta cell survival

As our data indicate that GPER signalling triggers beta cell apoptosis via downstream activation of ERα and ERβ, we sought to examine this hypothesis. First, we observed that G1-induced apoptosis was abolished by the antioestrogen ICI 182,780 (Fig. 5a,b). As G1 may also bind to and activate a 36-kDa variant of ERα, ERα36 [34], we silenced GPER (Fig. 5c, ESM Fig. 7a) to test whether G1 affected apoptosis via GPER. Notably, G1 did not affect apoptosis in GPER-silenced cells (Fig. 5d, ESM Fig. 7b), indicating that, in our cell system, G1 acts preferentially through GPER. Moreover, MPP (ERα antagonist) and PHTPP (ERβ antagonist) prevented G1-induced apoptosis (Fig. 5e-h). We then tested G1

effects on apoptosis upon silencing of ERα or ERβ separately (si*Erα* and si*Erβ*) or simultaneously (si*Erα*/*Erβ*) (Fig. 5i, ESM Fig. 7c-e). As described above, ERα or ERβ knockdown induced beta cell death and silencing of both receptors simultaneously induced apoptosis to the same extent observed in ERβ-inhibited cells (Fig. 5i, ESM Fig. 7f). G1 effect on apoptosis was lost in ERα-, ERβ- or ERα/ERβ-deficient cells (Fig. 5i, ESM Fig. 7f). Lastly, G1 induced apoptosis in dispersed islet cells from WT mice but its effect on apoptosis was completely blunted in dispersed cells from BERKO mice (Fig. 5j). These results indicate that ERβ seems to be more important than ERα for beta cell survival and that ERα and ERβ are required for GPER effects on viability.

ER heterodimerization

After ligand binding, ERα and ERβ form homodimers and heterodimers to exert their biological actions [10, 35]. As our data suggest that part of the BPA effect on apoptosis is directly mediated by ERα and ERβ, we sought to study if the binding of E2 or BPA would stabilize ER homo- and/or heterodimers. We performed docking and molecular dynamics simulations using human structural models of ERα and ERβ. Our models were obtained from resolved dimeric structures of the ER LBD where the protein is co-crystallized with ligands, E2 and BPA, bound to the LBD cavity that is closed by the transactivation helix H12 (Fig. 6a-c). Figure 6 depicts models of the ERα-ERα homodimer (ERαα; Fig. 6a), ERβ-ERβ homodimer (ERββ; Fig. 6b) and ERα-ERβ heterodimer (ERαβ; Fig. 6c).

Molecular docking simulations resulted in lower Gibbs free energy changes for E2 (-11.05 and -10.86 kcal/mol for hERα-LBD and hERβ-LBD, respectively) compared with BPA (-8.15 and -8.37 kcal/mol for hERα-LBD and hERβ-LBD, respectively). These values are similar to those observed for rat ERs [22] and agree with the higher affinity of both receptors for E2 (compared with BPA) [36]. We used these protein-ligand complexes as the starting point to initiate molecular dynamics simulations of the ligands within the cavity during 200 ns. Then, we analysed the monomer-monomer interaction energy (Fig. 6d-f), the trajectory of the ligands within the LBD pocket (ESM Fig. 8) and the solvation binding energy of E2 and BPA bound to the LBD cavity (Fig. 6g-i).

When we examined the monomer-monomer interaction energy with E2 or BPA bound to both cavities of the LBD, we found that, for ERαα homodimers, the frequency distribution of the intermolecular interaction energy between monomers was lower for E2 than for BPA (Fig. 6d). This indicates that E2 stabilizes ERαα homodimer more than BPA. For

ERββ homodimers, E2 and BPA presented a similar interaction energy, suggesting a comparable ERββ stabilization with both ligands (Fig. 6e). When the interaction energy for ERαβ heterodimers was analysed, E2 presented a much lower interaction energy than BPA, indicating that BPA does not stabilize heterodimers (Fig. 6f). The trajectory of E2 and BPA within the cavity behaves differently; E2 showed minimal deviations during the 200 ns simulation time for both homodimers and for the heterodimer (ESM Fig. 8), suggesting a high stability of the hormone within the LBD pocket in the homo- and heterodimers. Conversely, BPA shows rapid structural rearrangements for both homodimers and heterodimers (ESM Fig. 8), a behaviour previously showed for monomers [22, 37]. This suggests a less stable binding of BPA compared to E2 for the three configurations of dimers.

To investigate the binding affinity of both ligands in homo- and heterodimers we analysed the frequency distribution of the solvation binding energy values of E2 and BPA bound to each type of dimer [38] (Fig. 6g-i). Of note, positive values indicate strong ligand-protein binding [22]. E2 binding to both homodimer cavities, LBD-ERαα (Fig. 6g) and LBD-ERββ (Fig. 6h), shows very similar values. In the heterodimer, however, the solvation energy values were higher for E2 binding to the ERα monomer forming the heterodimer (75 kcal/mol) than for E2 binding to the ERβ monomer of the heterodimer (63 kcal/mol) (Fig. 6i). For BPA, the solvation binding energy values for homodimers were 30-35 kcal/mol for LBD-ERαα (Fig. 6g) and 55-60 kcal/mol for LBD-ERββ (Fig. 6i), which indicates that BPA showed higher affinity for ERββ than for ERαα. When we analysed the LBD-ERαβ, the frequency distribution of the solvation energy deviates from a Gaussian distribution, especially for BPA bound to the beta subunit of the heterodimer (Fig. 6i). This suggests a much lower BPA affinity for LBD-ERαβ compared with LBD-ERββ. In summary, these simulations indicate that BPA affinity is higher for ERββ than for ERαα and ERαβ. Binding of E2 should stabilize the three forms, preferentially ERαα, while BPA would mainly stabilize ERββ, to a much less extent ERαα and does not stabilize ERαβ.

To further explore how E2, BPA and G1 affect heterodimer formation we performed in situ proximity ligand assay (PLA) and co-immunoprecipitation. The PLA analysis showed a small number of heterodimers (shown as red dots) in vehicle-treated cells, which greatly increased upon E2 exposure for 24 h (Fig. 7a, Veh and E2 panels). In the presence of BPA or G1, however, very few red dots were observed, suggesting that these compounds decreased heterodimer formation (Fig. 7a, BPA and G1 panels). Co-

immunoprecipitation assay indicated that ERα directly bound to ERβ (Fig. 7b-e). In agreement with the PLA data, the interaction between ERα and ERβ was augmented by E2 and significantly reduced by BPA (Fig. 7b,c) and G1 (Fig. 7d,e). Altogether, these results suggest that E2 promotes ERαβ heterodimerization while BPA and G1 seemed to disrupt ERαβ formation.

Discussion

BPA is an endocrine disruptor with diabetogenic properties [17, 18]. In adult mice, BPA increases serum insulin levels and induces insulin resistance [15]. When administered to pregnant mice, BPA altered insulin release and beta cell mass in male offspring [16, 39] and in mothers later in life [16, 40]. Epidemiological studies have linked BPA exposure to type 2 diabetes development [41, 42]. Here we show that environmentally relevant doses of BPA increase beta cell apoptosis in an ERα-, ERβ- and GPER-dependent manner. Moreover, molecular dynamic simulations together with PLA and co-immunoprecipitation data indicate that BPA binding to ERα and ERβ as well as GPER activation decreased ERαβ heterodimers.

It has been shown that E2 protects beta cells from several pro-apoptotic stimuli, such oxidative stress [13], proinflammatory cytokines [43] and high glucose [44]. These studies suggest that ERα is crucial for pancreatic islet survival. For instance, E2 prevented streptozotocin-induced beta cell apoptosis in vivo and protected mice from insulin-deficient diabetes in an ERα-dependent manner [13]. Furthermore, ERα preserved mitochondrial function and attenuated endoplasmic reticulum stress in a context where ERα silencing promoted ROS production and induced beta cell apoptosis [45]. Here we showed similar findings. ERα knockdown or treatment with the ERα antagonist MPP induced beta cell apoptosis, reinforcing an antiapoptotic role of this receptor even in the absence of ligands. In the presence of ER ligands, we observed two different scenarios: while an ERα agonist had no effect on viability, BPA induced ROS production and beta cell apoptosis, indicating that BPA disrupts ERα antiapoptotic role. Our findings indicate that ERβ also plays a pro-survival role in beta cells, as either its silencing or antagonism with PHTPP leads to apoptosis. Interestingly, the percentage of apoptosis in ERβ-silenced cells were much higher than in ERα-deficient cells, suggesting that ERβ seems to be more important for beta cell survival. BPA effect on apoptosis was abrogated in ERβ-inhibited cells, indicating that, as for ERα, ERβ is also involved in BPA-induced apoptosis. The

antiapoptotic protection conferred by ERs is in line with previous findings in islets from ERα and ERβ knockout mice [12].

After ligand binding, ERα and ERβ form homo- and heterodimers to perform their biological effects [10]. Different ER ligands stabilize ERα and ERβ homo- and heterodimers in a variety of combinations that mediate the effect of those ER ligands [46]. BPA has a low affinity according to binding experiments and presents a low transcriptional effect when acting via the classical nuclear pathway [36, 47]. However, it induces apoptosis even at low doses. Our bioinformatic results predicted that E2 favours the formation of ERαα, ERββ and ERαβ. BPA, however, stabilized ERββ but did not stabilize ERαβ heterodimers. Based on these results we proposed a model where, in basal conditions, ERαα, ERββ and ERαβ are antiapoptotic. Upon binding, E2 would favour ERαβ heterodimers as well as ERαα and ERββ homodimers, thus protecting beta cells from apoptosis. Conversely, ERαβ heterodimer formation does not occur in the presence of BPA; in fact, the number of ERαβ heterodimers is even decreased by BPA exposure. Therefore, as one of the three ER branches promoting survival is missing, there is an increase in apoptosis (Fig. 8).

A direct effect of BPA on ERα and ERβ heterodimerization might explain the part of the BPA apoptotic effect that is neither blocked by GPER antagonism nor fully achieved by GPER activation. Nonetheless, we demonstrated that GPER activation by either BPA or G1 contributes to beta cell apoptosis. As BPA binds to GPER in other cell systems [48] and induces rapid nongenomic effects [49], it is plausible to assume that BPA acts as a GPER agonist in beta cells. As G1 and BPA effects were abolished in the presence of an ER antagonist, after ER knockdown and in islets cells from BERKO mice, we suggest that ERα and ERβ are responsible for the effect of GPER activation. A crosstalk between GPER and ERα has been described for E2 and environmental oestrogens [50]. Remarkably, E2, which also binds to and activates GPER [8, 9], does not behave as G1 or BPA. Although these differences remain elusive, our data indicate that they might be related to the E2-induced increase in ERαβ heterodimer formation (Fig. 8).

Thus, along with BPA effects on insulin secretion and insulin sensitivity, BPA-induced apoptosis described by us (present data) and others [24, 25] might contribute to elucidate the diabetogenic effects of BPA described above. Furthermore, uncovering a mechanism that involves GPER activation may help to explain the effects at low dose observed by low-affinity ER ligands like BPA.

Acknowledgements

The authors thank Maria Luisa Navarro, Salomé Ramon, and Beatriz Bonmati Botella for their excellent technical assistance. We are grateful to the Cluster of Scientific Computing (http://ccc.umh.es/) of the Universitas Miguel Hernández for providing computing facilities.

Data availability

Funding

This work was supported by Ministerio de Ciencia e Innovación, Agencia Estatal de Investigación (AEI) and Fondo Europeo de Desarrollo Regional (FEDER) grants BPU2017-86579-R (AN), PID2020-117294RB-I00 (AN, JM-P), Generalitat Valenciana PROMETEO II/2020/006 (AN) and European Union's Horizon 2020 research and innovation programme under grant agreement GOLIATH No. 825489 (AN). Author laboratories hold grants from Ministerio de Ciencia e Innovación, Agencia Estatal de Investigación y Fondo Europeo de Desarrollo Regional (FEDER) RTI2018-096724-B-C21 (J-AE) and PID2020-117569RA-I00 (LM). PROMETEO/2016/006 (J-AE) and SEJI/2018/023 (LM) supported by Generalitat Valenciana, Spain. Robert A. Welch Foundation (grant E-0004) (J-AG). CIBERDEM is an initiative of the Instituto de Salud Carlos III.

Duality of interests

The authors declare that there is no duality of interest associated with this manuscript.

Author contributions

LM and AN conceived the study. IB-C, RSDS, RMM-G, AAP-S, J-AE and LM collected and analysed the data. IB-C, RSDS, RMM-G, AAP-S, J-AE, JM-P, LM and AN interpreted the data. RSDS, JM-P and AN drafted the manuscript. AN and LM supervised the study. RSDS, JM-P, J-AG critically revised the manuscript for important intellectual content. J-AG, J-AE, LM, JM-P and AN acquired the funding. All authors reviewed and approved the final version of the manuscript, and gave consent to publication. LM and AN are responsible for the integrity of the work as a whole.

References

1. Eizirik DL, Pasquali L, Cnop M (2020) Pancreatic beta-cells in type 1 and type 2 diabetes mellitus: different pathways to failure. Nat Rev Endocrinol 16(7):349–362. https://doi.org/10.1038/s41574-020-0355-7

2. Gannon M, Kulkarni RN, Tse HM, Mauvais-Jarvis F (2018) Sex differences underlying pancreatic islet biology and its dysfunction. Mol Metab 15:82–91. https://doi.org/10.1016/j.molmet.2018.05.017

3. Kautzky-Willer A, Harreiter J, Pacini G (2016) Sex and Gender Differences in Risk, Pathophysiology and Complications of Type 2 Diabetes Mellitus. Endocr Rev 37(3):278–316. https://doi.org/10.1210/er.2015-1137

4. Basu R, Dalla Man C, Campioni M, et al (2006) Effects of age and sex on postprandial glucose metabolism: differences in glucose turnover, insulin secretion, insulin action, and hepatic insulin extraction. Diabetes 55(7):2001–2014. https://doi.org/10.2337/db05-1692

5. Hall E, Volkov P, Dayeh T, et al (2014) Sex differences in the genome-wide DNA methylation pattern and impact on gene expression, microRNA levels and insulin secretion in human pancreatic islets. Genome Biol 15(12):522. https://doi.org/10.1186/s13059-014-0522-z

6. Li T, Jiao W, Li W, Li H (2016) Sex effect on insulin secretion and mitochondrial function in pancreatic beta cells of elderly Wistar rats. Endocr Res 41(3):167–179. https://doi.org/10.3109/07435800.2015.1124437

7. Heldring N, Pike A, Andersson S, et al (2007) Estrogen receptors: how do they signal and what are their targets. Physiol Rev 87(3):905–931. https://doi.org/10.1152/physrev.00026.2006

8. Revankar CM, Cimino DF, Sklar LA, Arterburn JB, Prossnitz ER (2005) A transmembrane intracellular estrogen receptor mediates rapid cell signaling. Science 307(5715):1625–1630. https://doi.org/10.1126/science.1106943

9. Thomas P, Pang Y, Filardo EJ, Dong J (2005) Identity of an estrogen membrane receptor coupled to a G protein in human breast cancer cells. Endocrinology 146(2):624–632. https://doi.org/10.1210/en.2004-1064

10. Levin ER, Hammes SR (2016) Nuclear receptors outside the nucleus: extranuclear signalling by steroid receptors. Nat Rev Mol Cell Biol 17(12):783–797. https://doi.org/10.1038/nrm.2016.122

11. Balhuizen A, Kumar R, Amisten S, Lundquist I, Salehi A (2010) Activation of G protein-coupled receptor 30 modulates hormone secretion and counteracts cytokine-induced apoptosis in pancreatic islets of female mice. Molecular and Cellular Endocrinology 320(1–2):16–24. https://doi.org/10.1016/j.mce.2010.01.030

12. Liu S, le May C, Wong WP, et al (2009) Importance of extranuclear estrogen receptor-alpha and membrane G protein-coupled estrogen receptor in pancreatic islet survival. Diabetes 58(10):2292–2302. https://doi.org/10.2337/db09-0257

13. le May C, Chu K, Hu M, et al (2006) Estrogens protect pancreatic beta-cells from apoptosis and prevent insulin-deficient diabetes mellitus in mice. Proc Natl Acad Sci U S A 103(24):9232–9237. https://doi.org/10.1073/pnas.0602956103

14. Gore AC, Chappell VA, Fenton SE, et al (2015) EDC-2: The Endocrine Society's Second Scientific Statement on Endocrine-Disrupting Chemicals. Endocrine Reviews 36(6). https://doi.org/10.1210/er.2015-1010

15. Alonso-Magdalena P, Morimoto S, Ripoll C, Fuentes E, Nadal A (2006) The estrogenic effect of bisphenol A disrupts pancreatic beta-cell function in vivo and induces insulin resistance. Environ Health Perspect 114(1):106–112. https://doi.org/10.1289/ehp.8451

16. Alonso-Magdalena P, Vieira E, Soriano S, et al (2010) Bisphenol A exposure during pregnancy disrupts glucose homeostasis in mothers and adult male offspring. Environ Health Perspect 118(9):1243–1250. https://doi.org/10.1289/ehp.1001993

17. Alonso-Magdalena P, Quesada I, Nadal A (2011) Endocrine disruptors in the etiology of type 2 diabetes mellitus. Nat Rev Endocrinol 7(6):346–353. https://doi.org/10.1038/nrendo.2011.56

18. Sargis RM, Simmons RA (2019) Environmental neglect: endocrine disruptors as underappreciated but potentially modifiable diabetes risk factors. Diabetologia 62(10):1811–1822. https://doi.org/10.1007/s00125-019-4940-z

19. Vandenberg LN, Chahoud I, Heindel JJ, Padmanabhan V, Paumgartten FJ, Schoenfelder G (2010) Urinary, circulating, and tissue biomonitoring studies indicate widespread exposure to bisphenol A. Environ Health Perspect 118(8):1055–1070. https://doi.org/10.1289/ehp.0901716

20. Alonso-Magdalena P, Ropero AB, Carrera MP, et al (2008) Pancreatic insulin content regulation by the estrogen receptor ER alpha. PLoS One 3(4):e2069. https://doi.org/10.1371/journal.pone.0002069

21. Martinez-Pinna J, Marroqui L, Hmadcha A, et al (2019) Oestrogen receptor beta mediates the actions of bisphenol-A on ion channel expression in mouse pancreatic beta cells. Diabetologia 62(9):1667–1680. https://doi.org/10.1007/s00125-019-4925-y

22. Marroqui L, Martinez-Pinna J, Castellano-Munoz M, et al (2021) Bisphenol-S and Bisphenol-F alter mouse pancreatic beta-cell ion channel expression and activity and insulin release through an estrogen receptor ERbeta mediated pathway. Chemosphere 265:129051. https://doi.org/10.1016/j.chemosphere.2020.129051

23. Soriano S, Alonso-Magdalena P, Garcia-Arevalo M, et al (2012) Rapid insulinotropic action of low doses of bisphenol-A on mouse and human islets of Langerhans: role of estrogen receptor beta. PLoS One 7(2):e31109. https://doi.org/10.1371/journal.pone.0031109

24. Lin Y, Sun X, Qiu L, et al (2013) Exposure to bisphenol A induces dysfunction of insulin secretion and apoptosis through the damage of mitochondria in rat insulinoma (INS-1) cells. Cell Death Dis 4:e460. https://doi.org/10.1038/cddis.2012.206

25. Carchia E, Porreca I, Almeida PJ, et al (2015) Evaluation of low doses BPA-induced perturbation of glycemia by toxicogenomics points to a primary role of pancreatic islets and to the mechanism of toxicity. Cell Death and Disease 6(10). https://doi.org/10.1038/cddis.2015.319

26. Krege JH, Hodgin JB, Couse JF, et al (1998) Generation and reproductive phenotypes of mice lacking estrogen receptor β. Proceedings of the National Academy of Sciences of the United States of America 95(26). https://doi.org/10.1073/pnas.95.26.15677

27. Santin I, dos Santos RS, Eizirik DL (2016) Pancreatic beta cell survival and signaling pathways: Effects of type 1 diabetes-associated genetic variants. In: Methods in Molecular Biology

28. Ravassard P, Hazhouz Y, Pechberty S, et al (2011) A genetically engineered human pancreatic β cell line exhibiting glucose-inducible insulin secretion. Journal of Clinical Investigation 121(9). https://doi.org/10.1172/JCI58447

29. Cunha DA, Cito M, Carlsson PO, et al (2016) Thrombospondin 1 protects pancreatic β-cells from lipotoxicity via the PERK-NRF2 pathway. Cell Death and Differentiation 23(12). https://doi.org/10.1038/cdd.2016.89

30. Iwabuchi E, Miki Y, Ono K, et al (2017) In situ detection of estrogen receptor dimers in breast carcinoma cells in archival materials using proximity ligation assay (PLA). J Steroid Biochem Mol Biol 165(Pt B):159–169. https://doi.org/10.1016/j.jsbmb.2016.05.022

31. Biasini M, Bienert S, Waterhouse A, et al (2014) SWISS-MODEL: Modelling protein tertiary and quaternary structure using evolutionary information. Nucleic Acids Research 42(W1). https://doi.org/10.1093/nar/gku340

32. Tovchigrechko A, Vakser IA (2006) GRAMM-X public web server for protein-protein docking. Nucleic Acids Research 34(WEB. SERV. ISS.). https://doi.org/10.1093/nar/gkl206

33. Delgado J, Radusky LG, Cianferoni D, Serrano L (2019) FoldX 5.0: Working with RNA, small molecules and a new graphical interface. Bioinformatics 35(20). https://doi.org/10.1093/bioinformatics/btz184

34. Kang L, Zhang X, Xie Y, et al (2010) Involvement of estrogen receptor variant ER-alpha36, not GPR30, in nongenomic estrogen signaling. Mol Endocrinol 24(4):709–721. https://doi.org/10.1210/me.2009-0317

35. Razandi M, Pedram A, Merchenthaler I, Greene GL, Levin ER (2004) Plasma membrane estrogen receptors exist and functions as dimers. Mol Endocrinol 18(12):2854–2865. https://doi.org/10.1210/me.2004-0115

36. Kuiper GG, Carlsson B, Grandien K, et al (1997) Comparison of the ligand binding specificity and transcript tissue distribution of estrogen receptors alpha and beta. Endocrinology 138(3):863–870. https://doi.org/10.1210/endo.138.3.4979

37. Li Y, Perera L, Coons LA, et al (2018) Differential in vitro biological action, coregulator interactions, and molecular dynamic analysis of bisphenol A (BPA), BPAF, and BPS ligand–ERα complexes. Environmental Health Perspectives 126(1). https://doi.org/10.1289/EHP2505

38. Wang C, Nguyen PH, Pham K, et al (2016) Calculating protein-ligand binding affinities with MMPBSA: Method and error analysis. J Comput Chem 37(27):2436–2446. https://doi.org/10.1002/jcc.24467

39. Bansal A, Rashid C, Xin F, et al (2017) Sex- and dose-specific effects of maternal bisphenol A exposure on pancreatic islets of first- and second-generation adult mice offspring. Environmental Health Perspectives 125(9). https://doi.org/10.1289/EHP1674

40. Alonso-Magdalena P, García-Arévalo M, Quesada I, Nadal Á (2015) Bisphenol-A treatment during pregnancy in mice: A new window of susceptibility for the development of diabetes in mothers later in life. Endocrinology (United States) 156(5). https://doi.org/10.1210/en.2014-1952

41. Wang B, Li M, Zhao Z, et al (2019) Urinary bisphenol A concentration and glucose homeostasis in non-diabetic adults: a repeated-measures, longitudinal study. Diabetologia 62(9):1591–1600. https://doi.org/10.1007/s00125-019-4898-x

42. Rancière F, Botton J, Slama R, et al (2019) Exposure to bisphenol a and bisphenol s and incident type 2 diabetes: A case-cohort study in the French cohort D.E.S.I.R. Environmental Health Perspectives 127(10). https://doi.org/10.1289/EHP5159

43. Contreras JL, Smyth CA, Bilbao G, Young CJ, Thompson JA, Eckhoff DE (2002) 17β-estradiol protects isolated human pancreatic islets against proinflammatory cytokine-induced cell death: Molecular mechanisms and islet functionality. Transplantation 74(9). https://doi.org/10.1097/00007890-200211150-00010

44. Kooptiwut S, Kaewin S, Semprasert N, et al (2018) Estradiol Prevents High Glucose-Induced β-cell Apoptosis by Decreased BTG2 Expression. Scientific Reports 8(1). https://doi.org/10.1038/s41598-018-30698-x

45. Zhou Z, Ribas V, Rajbhandari P, et al (2018) Estrogen receptor protects pancreatic -cells from apoptosis by preserving mitochondrial function and suppressing endoplasmic reticulum stress. Journal of Biological Chemistry 293(13):4735–4751. https://doi.org/10.1074/jbc.M117.805069

46. Paulmurugan R, Tamrazi A, Massoud TF, Katzenellenbogen JA, Gambhir SS (2011) In vitro and in vivo molecular imaging of estrogen receptor α and β homo- and heterodimerization: Exploration of new modes of receptor regulation. Molecular Endocrinology 25(12):2029–2040. https://doi.org/10.1210/me.2011-1145

47. Molina-Molina JM, Amaya E, Grimaldi M, et al (2013) In vitro study on the agonistic and antagonistic activities of bisphenol-S and other bisphenol-A congeners and derivatives via nuclear receptors. Toxicology and Applied Pharmacology 272(1). https://doi.org/10.1016/j.taap.2013.05.015

48. Thomas P, Dong J (2006) Binding and activation of the seven-transmembrane estrogen receptor GPR30 by environmental estrogens: A potential novel mechanism of endocrine disruption. Journal of Steroid Biochemistry and Molecular Biology 102(1-5 SPEC. ISS.):175–179. https://doi.org/10.1016/j.jsbmb.2006.09.017

49. Chevalier N, Paul-Bellon R, Camparo P, Michiels JF, Chevallier D, Fénichel P (2014) Genetic variants of GPER/GPR30, a novel estrogen-related G protein receptor, are associated with human seminoma. International Journal of Molecular Sciences 15(1):1574–1589. https://doi.org/10.3390/ijms15011574

50. Qie Y, Qin W, Zhao K, Liu C, Zhao L, Guo LH (2021) Environmental Estrogens and Their Biological Effects through GPER Mediated Signal Pathways. Environmental Pollution 278:116826. doi: 10.1016/j.envpol.2021.116826.

Figures

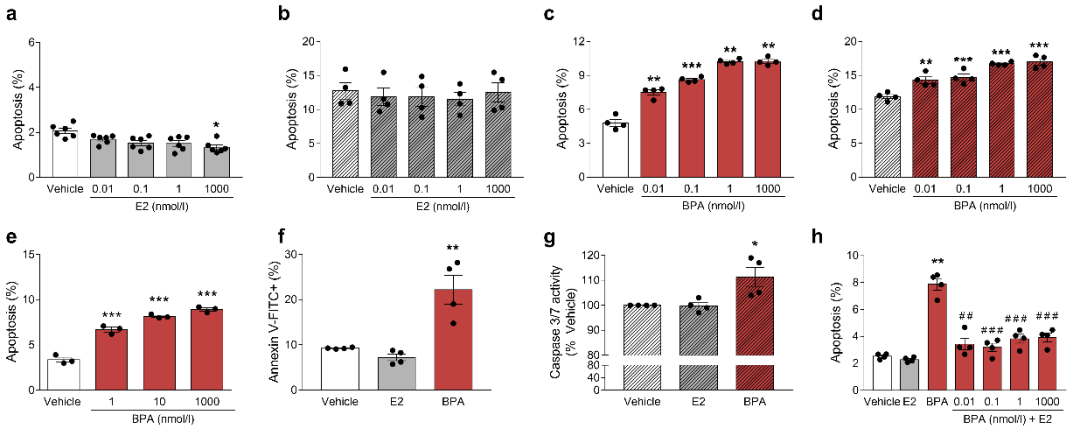

Fig. 1 E2 and BPA have different effects on beta cell viability. INS-1E (**a,c**) and EndoC-βH1 cells (**b,d**) were treated with vehicle (white bars), E2 (grey bars) or BPA (red bars) for 24 h. (**e**) Dispersed islet cells from female mice were treated with vehicle (white bars) or BPA (red bars) for 48 h. Apoptosis was evaluated using Hoechst 33342 and propidium iodide staining. (**f**) INS-1E cells were treated with vehicle (white bar), E2 1 nmol/l (grey bar) or BPA 1 nmol/l (red bar) for 48 h. Annexin V-FITC-positive cells were analysed by flow cytometry. (**g**) EndoC-βH1 cells were treated with vehicle (white bar), E2 1 nmol/l (grey bar) or BPA 1 nmol/l (red bar) for 48 h. Caspase 3/7 activity was measured by a luminescent assay. Results are expressed as % vehicle-treated cells. (**h**) INS-1E were treated with vehicle (white bar), E2 1 nmol/l (grey bar), BPA 1 nmol/l (red bar) or a combination of both (red bars + E2) for 24 h. Apoptosis was evaluated using Hoechst 33342 and propidium iodide staining. Data are shown as means ± SEM of 3-6 independent experiments. (**a-i**) $^{*}p \leq 0.05$, $^{**}p \leq 0.01$ and $^{***}p \leq 0.001$ vs Vehicle, by one-way ANOVA. (**h**) $^{**}p \leq 0.01$ vs Vehicle; $^{\#\#}p \leq 0.01$ and $^{\#\#\#}p \leq 0.001$ vs BPA 1 nmol/l. One-way ANOVA.

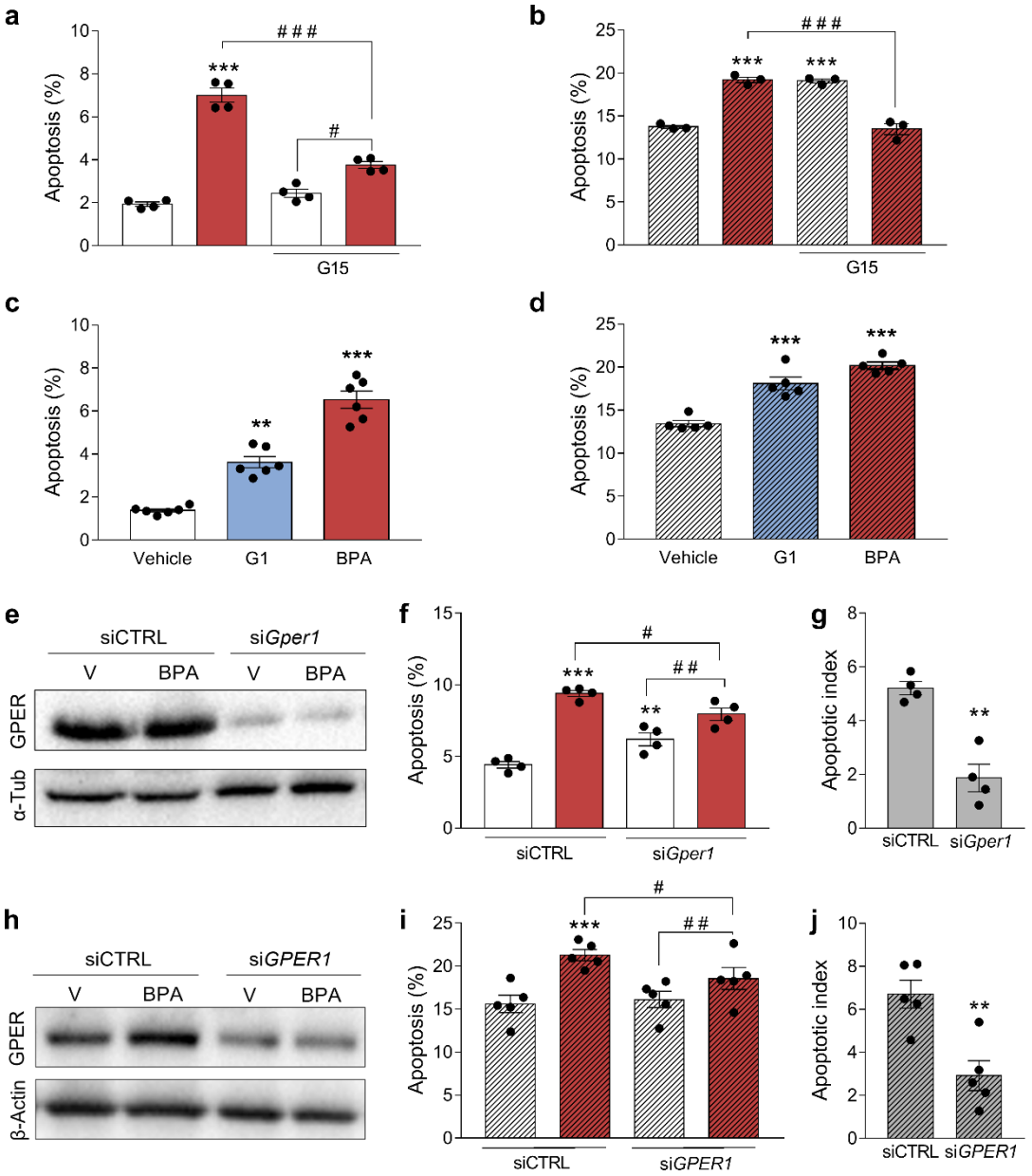

Fig. 2 BPA-induced apoptosis requires GPER. (**a,b**) INS-1E (**a**) and EndoC-βH1 cells (**b**) were pre-treated with vehicle or GPER antagonist G15 10 nmol/l for 3 h. Afterwards, cells were treated with vehicle (white bars) or BPA 1 nmol/l (red bars) in the absence or presence of G15 10 nmol/l for 24 h. (**c,d**) INS-1E (**c**) and EndoC-βH1 cells (**d**) were treated with vehicle (white bars), G1 100 nmol/l (blue bars) or BPA 1 nmol/l (red bars) for 24 h. Apoptosis was evaluated using Hoechst 33342 and propidium iodide staining. (**e-j**) INS-1E (**e-g**) and EndoC-βH1 cells (**h-j**) were transfected with siCTRL or with a siRNA targeting GPER (si*Gper1* or si*GPER1*). Cells were treated with vehicle (white bars) or BPA 1 nmol/l (red bars) for 24 h. (**e,h**) Protein expression was measured by

western blot. Representative images of four (**e**) or five (**h**) independent experiments are shown. (**f,i**) Apoptosis was evaluated using Hoechst 33342 and propidium iodide staining. (**g,j**) BPA-induced apoptosis data from Fig. 5f (**g**) and Fig. 5i (**j**) are presented as apoptotic index. Data are shown as means ± SEM of 4-6 independent experiments. (**a,b**) $^{**}p \leq 0.01$ and $^{***}p \leq 0.001$ vs untreated vehicle; $^{\#\#}p \leq 0.01$, $^{\#\#\#}p \leq 0.001$ as indicated by bars. Two-way ANOVA. (**c,d**) $^{**}p \leq 0.01$ and $^{***}p \leq 0.001$ vs vehicle, by one-way ANOVA. (**f,i**) $^{**}p \leq 0.01$ and $^{***}p \leq 0.001$ vs siCTRL vehicle; $^{\#}p \leq 0.05$ and $^{\#\#}p \leq 0.01$ as indicated by bars. Two-way ANOVA. (**g,j**) $^{**}p \leq 0.01$ vs siCTRL, by two-tailed Student's *t* test.

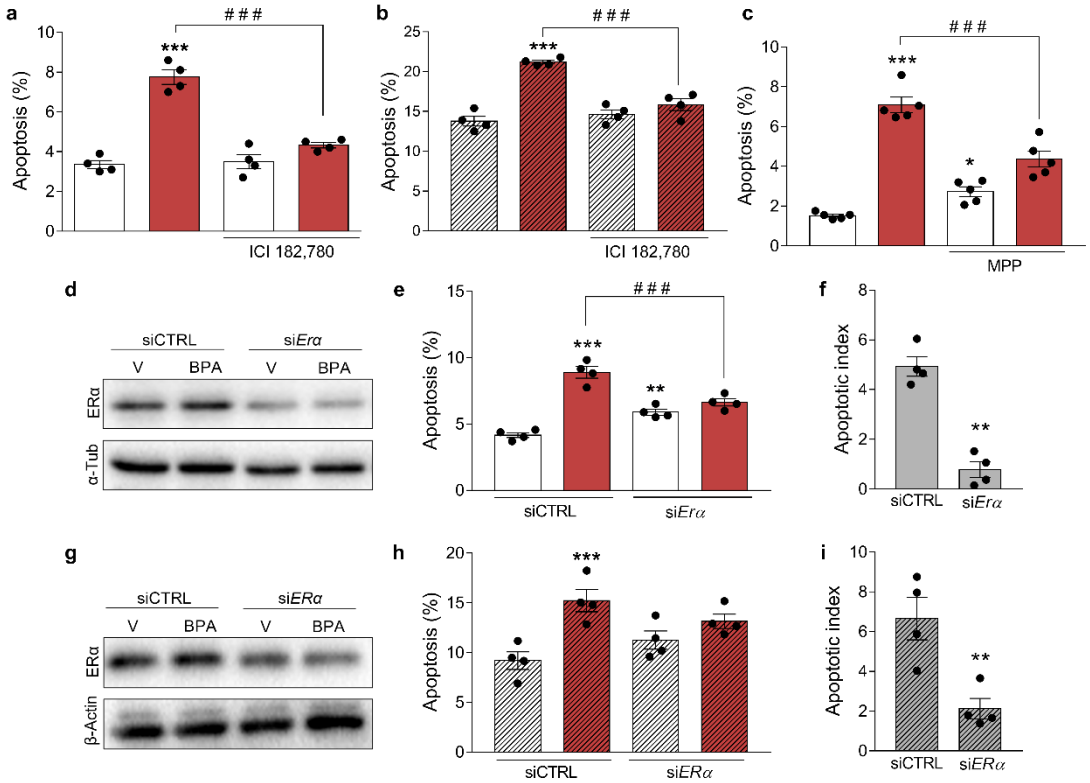

Fig. 3 ERα mediates BPA-induced apoptosis. (**a,b**) INS-1E (**a**) and EndoC-βH1 cells (**b**) were pre-treated with vehicle or antioestrogen ICI 182,780 1 µmol/l for 3 h. Afterwards, cells were treated with vehicle (white bars) or BPA 1 nmol/l (red bars) in the absence or presence of ICI 182,780 1 µmol/l for 24 h. (**c**) INS-1E cells were pre-treated with vehicle or ERα antagonist MPP 100 nmol/l for 3 h. Afterwards, cells were treated with vehicle (white bars) or BPA 1 nmol/l (red bars) in the absence or presence of MPP 100 nmol/l for 24 h. Apoptosis was evaluated using Hoechst 33342 and propidium iodide staining. (**d-i**) INS-1E (**d-f**) and EndoC-βH1 cells (**g-i**) were transfected with siCTRL or with a siRNA targeting ERα (si*Erα* or si*ERα*). Cells were treated with vehicle (white bars) or BPA 1 nmol/l (red bars) for 24 h. (**d,g**) Protein expression was measured by western blot. Representative images of four independent experiments are shown. (**e,h**) Apoptosis was evaluated using Hoechst 33342 and propidium iodide staining. (**g,j**) BPA-induced apoptosis data from Fig. 5e (**f**) and Fig. 5h (**i**) are presented as apoptotic index. Data are shown as means ± SEM of 4-5 independent experiments. (**a-c**) $^{*}p\leq0.05$ and $^{***}p\leq0.001$ vs untreated vehicle; $^{###}p\leq0.001$ as indicated by bars. Two-way ANOVA. (**e,h**) $^{**}p\leq0.01$ and $^{***}p\leq0.001$ vs siCTRL vehicle; $^{###}p\leq0.001$ as indicated by bars. Two-way ANOVA. (**f,i**) $^{**}p\leq0.01$ vs siCTRL, by two-tailed Student's *t* test.

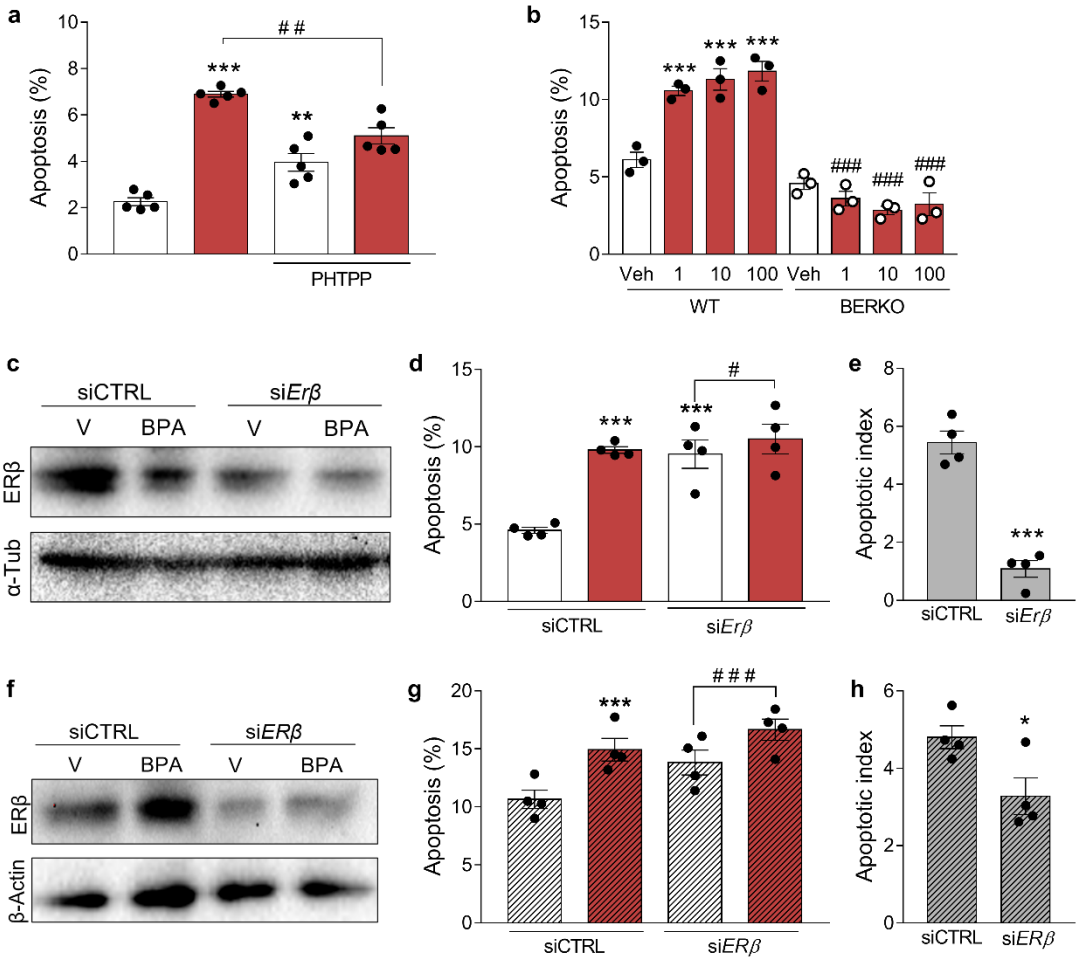

Fig. 4 ERβ mediates BPA-induced apoptosis. (**a**) INS-1E cells were pre-treated with vehicle or ERβ antagonist PHTPP 1 µmol/l for 3 h. Afterwards, cells were treated with vehicle (white bars) or BPA 1 nmol/l (red bars) in the absence or presence of PHTPP 1 µmol/l for 24 h. (**b**) Dispersed islet cells from WT and BERKO mice were treated with vehicle (white bars) or BPA (red bars) for 48 h. Apoptosis was evaluated using Hoechst 33342 and propidium iodide staining. (**c-h**) INS-1E (**c-e**) and EndoC-βH1 cells (**f-h**) were transfected with siCTRL or with a siRNA targeting ERβ (si*Erβ* or si*ERβ*). Cells were treated with vehicle (white bars) or BPA 1 nmol/l (red bars) for 24 h. (**c,f**) Protein expression was measured by western blot. Representative images of four independent experiments are shown. (**d,g**) Apoptosis was evaluated using Hoechst 33342 and propidium iodide staining. (**e,h**) BPA-induced apoptosis data from Fig. 5d (**e**) and Fig. 5g (**h**) are presented as apoptotic index. Data are shown as means ± SEM of 3-5 independent experiments. (**a**) $^{**}p\leq0.01$ and $^{***}p\leq0.001$ vs untreated vehicle; $^{\#\#}p\leq0.01$ as indicated by bars. Two-way ANOVA. (**b**) $^{***}p\leq0.001$ vs WT vehicle; $^{\#\#\#}p\leq0.001$ vs respective WT.

Two-way ANOVA. (**d,g**) ***$p \leq 0.001$ vs siCTRL vehicle; $^{\#}p \leq 0.05$ and $^{\#\#\#}p \leq 0.001$ as indicated by bars. Two-way ANOVA. (**e,h**) *$p \leq 0.05$ and ***$p \leq 0.001$ vs siCTRL, by two-tailed Student's *t* test.

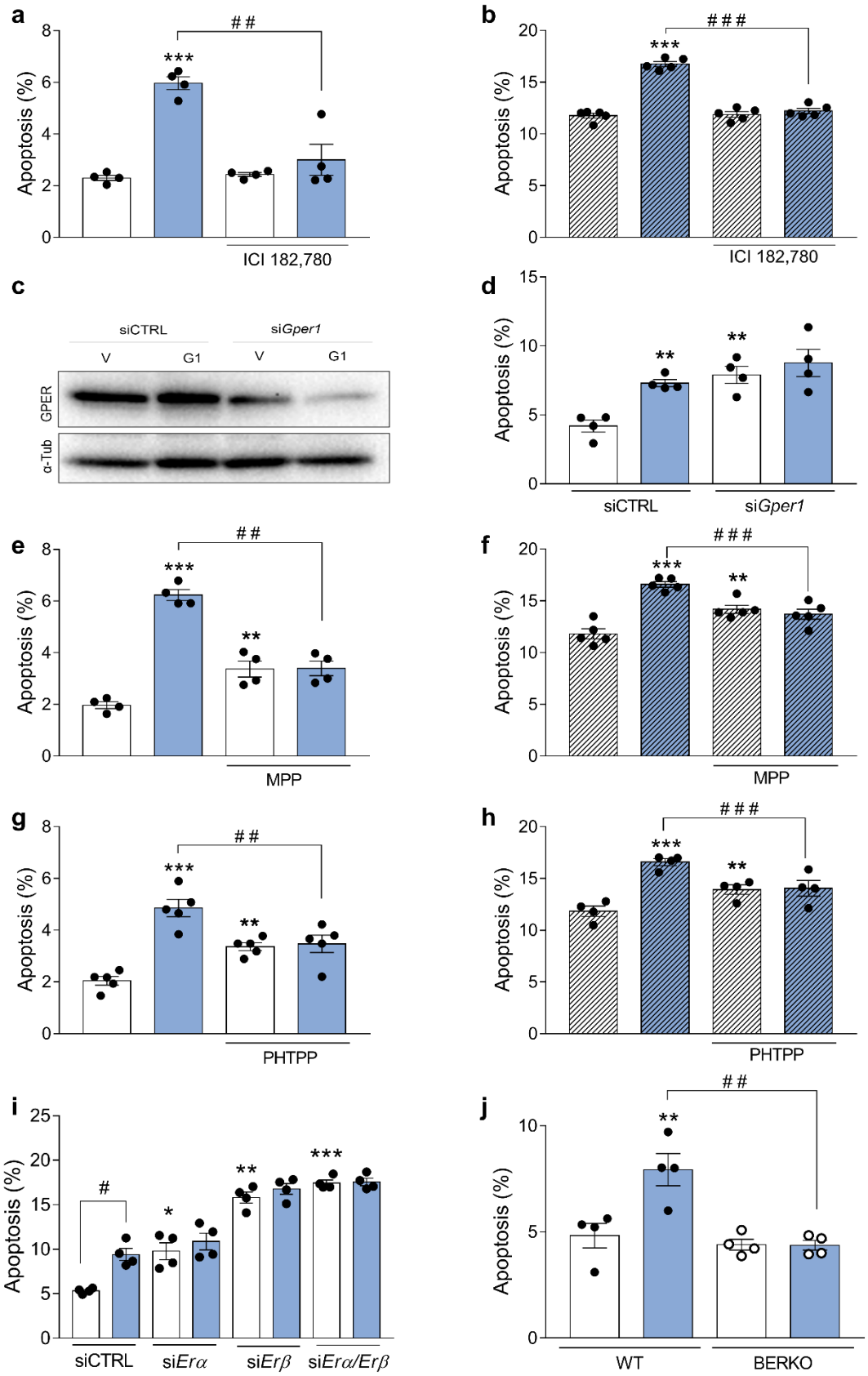

Fig. 5 A GPER crosstalk with ERα and ERβ induces apoptosis. (**a**,**b**) INS-1E (**a**) and EndoC-βH1 cells (**b**) were pre-treated with vehicle or antioestrogen ICI 182,780 1 µmol/l

for 3 h. Afterwards, cells were treated with vehicle (white bars) or G1 100 nmol/l (blue bars) in the absence or presence of ICI 182,780 1 μmol/l for 24 h. Apoptosis was evaluated using Hoechst 33342 and propidium iodide staining. (**c,d**) INS-1E were transfected with siCTRL or with a siRNA targeting GPER (si*Gper1*). Cells were treated with vehicle (white bars) or G1 100 nmol/l (blue bars) for 24 h. (**c**) Protein expression was measured by western blot. Representative images of four independent experiments are shown. (**d**) Apoptosis was evaluated using Hoechst 33342 and propidium iodide staining. (**e-h**) INS-1E (**e,g**) and EndoC-βH1 cells (**f,h**) were pre-treated with vehicle, ERα antagonist MPP 100 nmol/l (**e,f**) or ERβ antagonist PHTPP 1 μmol/l (**g,h**) for 3 h. Afterwards, cells were treated with vehicle (white bars) or G1 100 nmol/l (blue bars) in the absence or presence of MPP 100 nmol/l (**e,f**) or PHTPP 1 μmol/l (**g,h**) for 24 h. Apoptosis was evaluated using Hoechst 33342 and propidium iodide staining. (**g,h**) INS-1E cells were transfected with siCTRL or siRNAs targeting ERα (si*Erα*) and ERβ (si*Erβ*) or ERα and ERβ simultaneously (si*Erα*/*Erβ*.) Cells were treated with vehicle (white bars) or G1 100 nmol/l (blue bars) for 24 h. Apoptosis was evaluated using Hoechst 33342 and propidium iodide staining. (**e**) Dispersed islet cells from WT and BERKO mice were treated with vehicle (white bars) or G1 100 nM (blue bars) for 48 h. Apoptosis was evaluated using Hoechst 33342 and propidium iodide staining. Data are shown as means ± SEM of 4-5 independent experiments. (**a,b,e-h**) $^{**}p\leq0.01$ and $^{***}p\leq0.001$ vs untreated vehicle; $^{\#\#\#}p\leq0.001$ as indicated by bars. Two-way ANOVA. (**d,i**) $^{*}p\leq0.05$, $^{**}p\leq0.01$ and $^{***}p\leq0.001$ vs siCTRL vehicle; $^{\#}p\leq0.001$ as indicated by bars. Two-way ANOVA. (**j**) $^{**}p\leq0.01$ vs WT vehicle; $^{\#\#}p\leq0.01$ as indicated by bars. Two-way ANOVA.

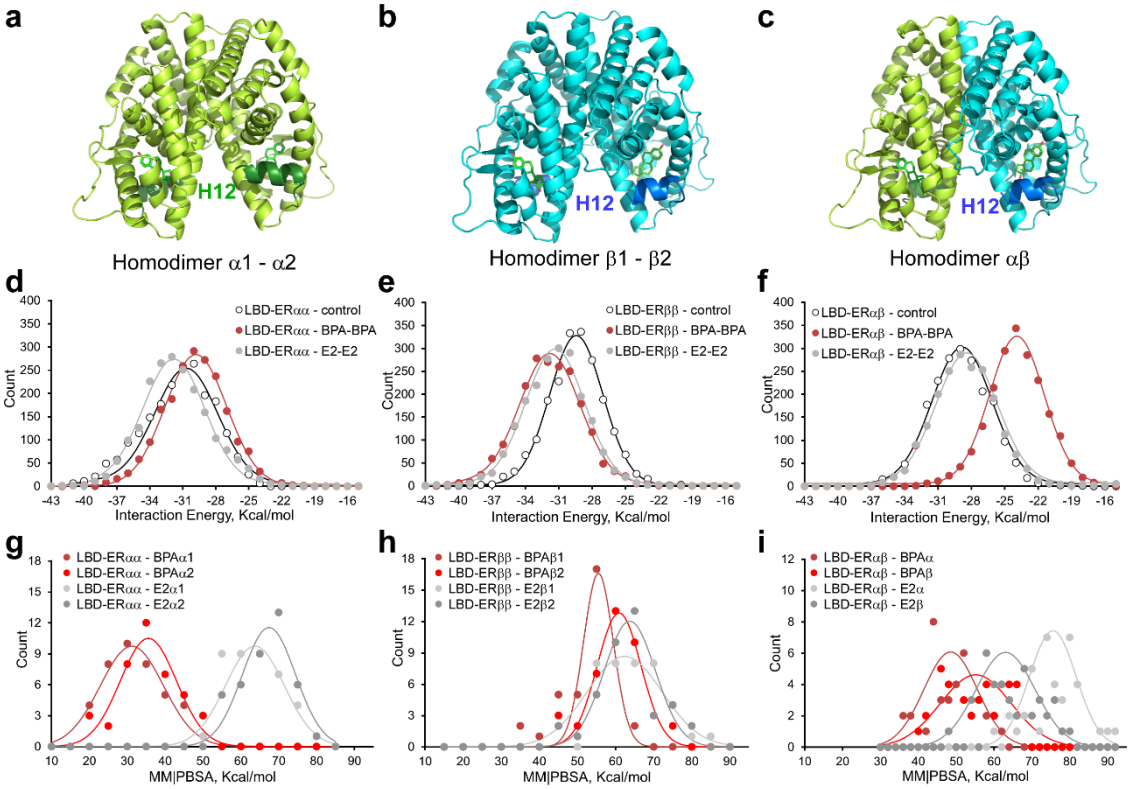

Fig. 6 Effect of BPA and E2 on the molecular dynamics for the LBD of the homodimer- or heterodimer-ER. Secondary structure models of closed LBD-ER as (**a**) alpha homodimer, (**b**) beta homodimer and (**c**) alpha-beta heterodimer. The H12 helix has been colored dark green (alpha monomers) or dark blue (beta monomers). The structure of E2 (green sticks for carbons) is included within the LBD cavities of both subunits. (**d**) Frequency distributions of the intermolecular protein Foldx-calculated interaction energy for the subunits of the alpha homodimer, (**e**) beta homodimer and (**f**) alfa-beta heterodimer in the presence of BPA or E2 ligands in each H12 closed LBD cavity. (**g**) Frequency distributions of the molecular mechanics Poisson–Boltzmann surface area (MM/PBSA) solvation binding energy values of each ligand bound to cavity of the alpha homodimer, (**h**) beta homodimer or (**i**) alpha-beta heterodimer in the presence of BPA or E2 ligands inside of the closed LBD. YASARA software-calculated MM|PBSA values more positive energies indicate better binding of the compound bound to the protein. A Gaussian curve overlaps discrete data.

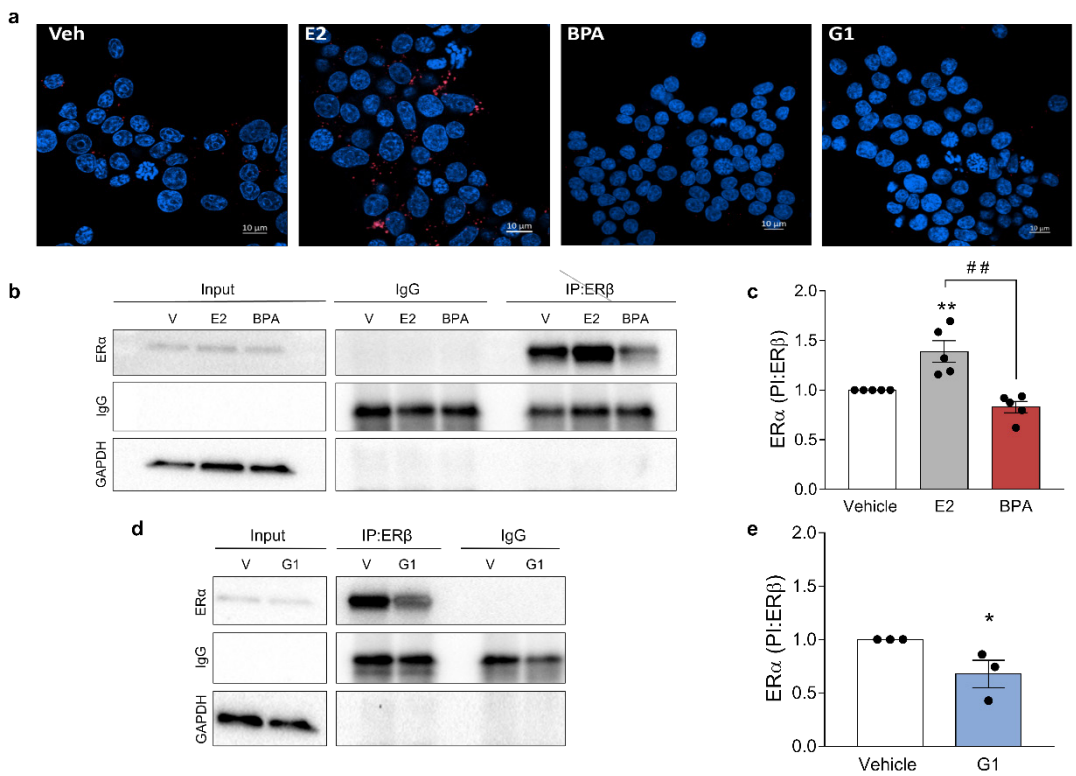

Fig. 7 E2 and BPA have differential effects on ERα/β heterodimer formation. (a) INS-1E cells were treated with vehicle, E2 1 nmol/l, BPA 1 nmol/l or G1 100 nmol/l for 24 h. Heterodimers were detected using in situ proximity ligand assay, where heterodimers are represented as red dots (Texas red) and nuclei are shown in blue (DAPI). (**b-e**) INS-1 E cells were treated with vehicle (white bars), E2 1 nmol/l (grey bars), BPA 1 nmol/l (red bars) (**b,c**) or G1 100 nmol/l (blue bars) (**d,e**) for 24 h. Cells were lysed and proteins collected for co-immunoprecipitation with anti-ERβ antibody. Nonspecific rabbit IgG was used as a negative control. Immunoprecipitates and total protein (Input) expression were measured by western blot. Representative images of three to five independent experiments are shown (**b,d**) and densitometry results are presented for ERα-specific binding to ERβ (**c,e**). Values were normalised by GAPDH and then by the value of vehicle-treated cells of each experiment (considered as 1). Data are shown as means ± SEM of 3-5 independent experiments. (**c**) $^{**}p \leq 0.01$ vs vehicle; $^{\#\#}p \leq 0.01$ as indicated by bars. One-way ANOVA. (**e**) $^{*}p \leq 0.05$ vs vehicle, by two-tailed Student's *t* test.

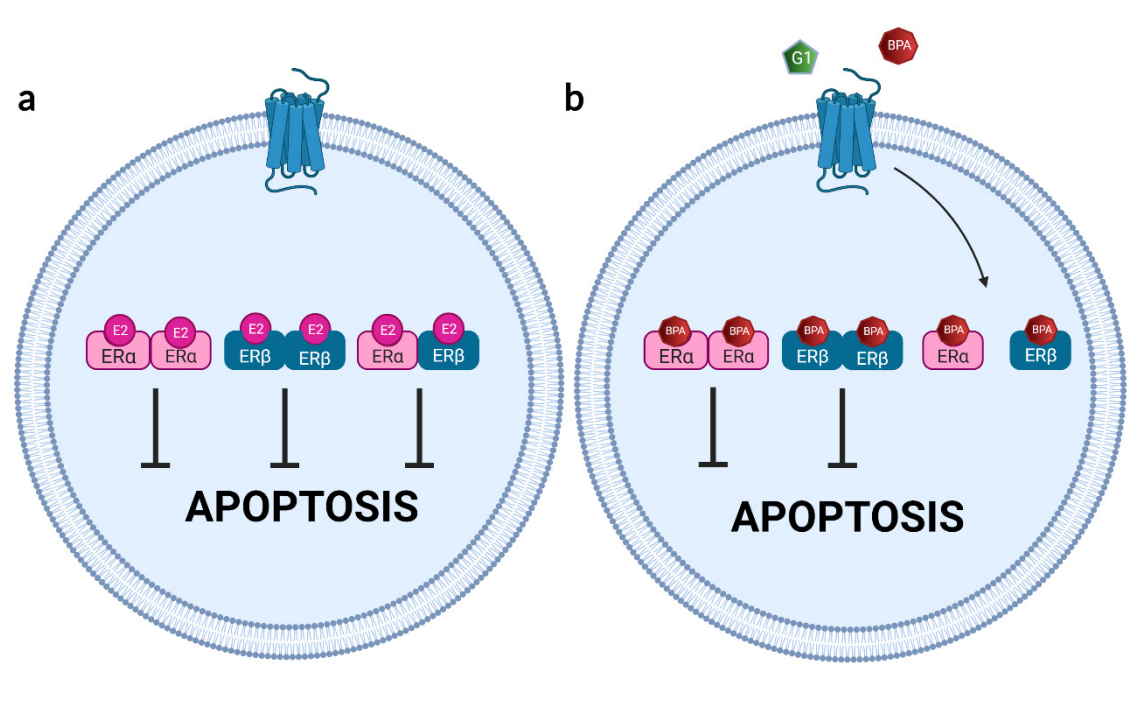

Fig. 8 Scheme summarizing our model for E2 and BPA induced effects on β-cells apoptosis. (**a**) In basal conditions ERα, ERβ homodimers and ERαβ heterodimers exist and protect from apoptosis, these dimers are also stabilized by E2. (**b**) Activation of GPER by G1 or BPA decreases ERαβ heterodimers and increases apoptosis. Binding of BPA to ERα and/or ERβ disfavors ERαβ formation. Created with BioRender.com.